Bifurcation and Transition of Multiple Charged One-Plus-Half Monopole Solutions of the SU(2) Yang-Mills-Higgs Theory

Dan Zhu, Khai-Ming Wong, and Timothy Tie

School of Physics, Universiti Sains Malaysia, 11800 USM Penang, Malaysia

(Received: 30.1.2018 ; Published: 7.6.2018)

Abstract. In this paper, we report on the electrically neutral one-plus-half monopole configuration of the SU(2) Yang-Mills-Higgs Theory when the ϕ-winding number, n, runs from 2 to 4 and for a range of Higgs coupling constant, $\lambda_b \leq \lambda \leq 40$, where λ_b is the lower bound, below which no solution can be found. Bifurcation and transition are observed when $n > 2$ and when the Higgs coupling constant is larger than some critical value, λ_c and λ_t, respectively. Two different branchings above the fundamental branch with higher energies for both $n = 3$ and 4 are observed. A new branch with even higher energies also emerged for $n = 4$. All solutions possess finite energy. Plots of magnetic charge density, Higgs modulus and energy density are presented and analyzed.

Keywords: SU(2) Yang-Mills-Higgs Theory, Monopole, Half-monopole

I. INTRODUCTION

The SU(2) Yang-Mills-Higgs theory possesses a large variety of monopole configurations and they have been studied extensively since mid-70s [1-5]. No exact monopole solution has been found when the Higgs field self-coupling constant, λ, is non-vanishing [1]. Many different numerical monopoles and antimonopoles solutions have been found. Among those, monopole-antimonopole pair (MAP), monopole-antimonopole chain (MAC), and vortex ring solutions are a few common types [6]. Most of monopole solutions reported in this field are of integer topological charges. However, the work done in this paper is based on previous findings of half-monopoles [7] and one-plus-half monopole solution [8]. The magnetic charge of the half-monopole is of opposite sign to that of the 't Hooft-Polyakov monopole [5]. This configuration possesses gauge potentials that are singular only along the z-axis.

Here, we further investigate the electrically neutral one-plus-half monopole solution when n = 2, 3 and 4 and for Higgs coupling constant, $\lambda_b < \lambda \leq 40$. The two branchings above the fundamental branch (FB) are labeled higher energy branch (HEB) and lower energy branch (LEB) and the new branch emerged when $n = 4$ is simply named new branch (NB) for later references. Transitions from multimonopole solutions to vortex ring solutions are observed in some branchings. λ_b, λ_c and λ_t are tabulated as well. Total energy, E and magnetic dipole moment, μ_m for different branchings is plotted against $\lambda^{1/2}$. Plots of Higgs modulus, magnetic charge density and energy density are also presented.

Contributed Paper

II. THE SU(2) YANG-MILLS-HIGGS THEORY

The Lagrangian in 3+1 dimensions with non-vanishing Higgs potential is given as:

$$\mathcal{L} = -(1/4)F^a_{\mu\nu}F^{a\mu\nu} - (1/2)D^\mu\Phi^a D_\mu\Phi^a - (1/4)\lambda[\Phi^a\Phi^a - (\mu^2/\lambda)]^2, \quad (1)$$

where $F^a_{\mu\nu}$ is the gauge field strength tensor. $D_\mu\Phi^a$ stands for the covariant derivative of the Higgs field, λ is the Higgs potential and ξ is defined as $\xi = \mu/\sqrt{\lambda}$, which is the expectation value of the Higgs field. Here μ is the Higgs field mass. The Lagrangian (1) is gauge invariant and stays unchanged under independent local SU(2) transformations. Parameter *a*, *b* and *c*, which are SU(2) internal group indices, run from 1 to 3, whereas μ and *v* are space-time indices of Minkowski space, run from 0 to 3.

The covariant derivative and gauge field strength tensor are given by:

$$D_\mu\Phi^a = \partial_\mu\Phi^a + g\varepsilon^{abc}A^b_\mu\Phi^c,\ F^a_{\mu\nu} = \partial_\mu A^a_\nu - \partial_\nu A^a_\mu + g\varepsilon^{abc}A^b_\mu A^c_\nu\ . \quad (2)$$

Here, g is gauge field coupling constant and A^a_μ is the gauge potential. Applying the Euler-Lagrange equation to Lagrangian (1), we obtain the equations of motion:

$$D^\mu F^a_{\mu\nu} = \partial^\mu F^a_{\mu\nu} + g\varepsilon^{abc}A^{b\mu}F^c_{\mu\nu} = g\varepsilon^{abc}\Phi^b D_\upsilon\Phi^c,\ D^\mu D_\mu\Phi^a = \lambda\Phi^a\left(\Phi^b\Phi^b - \xi^2\right). \quad (3)$$

The magnetic field, which can be decomposed into gauge and Higgs parts, are:

$$B_i = -(1/2)\varepsilon_{ijk}F_{jk} = B^G_i + B^H_i,\ B^G_i = -n\varepsilon_{ijk}\partial_j\sin\kappa\,\partial_j\phi,\ B^H_i = -n\varepsilon_{ijk}\partial^j\sin\alpha\,\partial^k\phi$$
$$\sin\kappa = (\sin\theta/n)[\psi_2(\Phi_2/|\Phi|) - R_2(\Phi_1/|\Phi|)], \sin\alpha = (\Phi_1/|\Phi|)\cos\theta - (\Phi_2/|\Phi|)\sin\theta \quad (4)$$

and thus the net magnetic charge of the system is: $M = (1/4\pi)\int\partial^i B_i d^3x = (1/4\pi)\oint d^2\,\sigma_i B_i$.

From Maxwell electromagnetic theory, 't Hooft's gauge potential (4) at large *r* tends to:

$$A_i = (\cos\alpha + \cos\kappa)\partial_i\varphi|_{r\to\infty} = (\hat{\varphi}_i/\mathrm{r}\sin\theta)[(1/2)\cos(\theta \pm 1) + (F_G(\theta)/r)]$$
$$F_G(\theta) = r\{(\Phi_2/|\Phi|)(P_1 - \sin\theta) - (\Phi_1/|\Phi|)(P_2 - \cos\theta) - (1/2)(\cos\theta \pm 1)\}|_{r\to\infty}. \quad (5)$$

The dimensionless magnetic dipole moment, μ_m, is obtained through the graph of $F_G(\theta)$ versus angle θ, related by the formula $F_G(\theta) = \mu_m\sin\theta$.

The dimensionless energy of the configuration is given by [9]:

$$E = (g/8\pi\xi)\int\{B^a_i B^a_i + D_i\Phi^a D_i\Phi^a + (\lambda/2)(\Phi^a\Phi^a - \xi^2)^2\}r^2\sin\theta\,drd\theta d\phi. \quad (6)$$

III. THE MAGNETIC ANSATZ

The magnetic ansatz [7] used in this paper in order to produce one-plus-half monopole is:

$$gA^a_i = -r^{-1}\psi_1(r,\theta)\hat{n}^a_\phi\hat{\theta}_i + (r\sin\theta)^{-1}P_1(r,\theta)\hat{n}^a_\theta\hat{\phi}_i + r^{-1}R_1(r,\theta)\hat{n}^a_\phi\hat{r}_i - (r\sin\theta)^{-1}P_2(r,\theta)\hat{n}^a_r\hat{\phi}_i$$
$$gA^a_0 = 0, g\Phi^a = \Phi_1(r,\theta)\hat{n}^a_r + \Phi_2(r,\theta)\hat{n}^a_\theta, \quad (7)$$

where $P_1 = \sin\theta\,\psi_2$, $P_2 = \sin\theta\,R_2$. $\hat{n}^a_r, \hat{n}^a_\theta, \hat{n}^a_\phi$ are unit vectors of the orthonormal isospin coordinate system and $\hat{r}_i, \hat{\theta}_i, \hat{\phi}_i$ are unit vectors of the spatial spherical coordinate systems.

The boundary conditions for *r*, when *r* approaches infinity are:

$$\psi_1 = 3/2\,, R_1 = 0, P_1 = n\sin\theta + (n/2)\sin(\theta/2)\,(1+\cos\theta)$$
$$P_2 = n\cos\theta - (n/2)\cos(\theta/2)\,(1+\cos\theta), \Phi_1 = \xi\cos(\theta/2)\,, \Phi_2 = \xi\sin(\theta/2). \quad (8)$$

Near the origin, we have the common trivial vacuum solution:

$$\psi_1 = P_1 = R_1 = P_2 = 0, \Phi_1 = \xi_0 \cos\theta\,, \Phi_2 = -\xi_0 \sin\theta$$
$$\sin\theta\,\Phi_1(0,\theta) + \cos\theta\,\Phi_2(0,\theta) = 0, \partial_r(\cos\theta\,\Phi_1(r,\theta) - \sin\theta\,\Phi_2(r,\theta))|_{r=0} = 0. \quad (9)$$

The corresponding boundary conditions imposed along the positive and negative *z*-axis for θ are as follows:

$$\partial_\theta\Phi_1(r,\theta)|_{\theta=0} = \Phi_2(r,0) = \partial_\theta\psi_1(r,\theta)|_{\theta=0} = R_1(r,0) = P_1(r,0) = \partial_\theta P_2(r,\theta)|_{\theta=0} = 0$$
$$\partial_\theta\Phi_1(r,\theta)|_{\theta=\pi} = \Phi_2(r,\pi) = \partial_\theta\psi_1(r,\theta)|_{\theta=\pi} = R_1(r,\pi) = P_1(r,\pi) = \partial_\theta P_2(r,\theta)|_{\theta=\pi} = 0\,. \quad (10)$$

Eq.(8)-(10) constitute the full set of boundary conditions for *r* and θ. Then, upon substituting the magnetic ansatz (7) into the equations of motion (3), the set of equations of motion are reduced to six coupled second order partial differential equations. Those equations are solved numerically with the given boundary conditions using Maple and MATLAB [11]. These six coupled second order partial differential equations were then transformed into a system of nonlinear equations using the finite difference approximation, and then discretized on a non-equidistant grid of size 110×100 covering the integration regions $0 \leq x \leq 1$ and $0 \leq \theta \leq \pi$. Here $x = r / (r + 1)$ is the finite interval compactified coordinate. Also, some constants, such as *g* and ξ were set to one in the process.

IV. RESULTS AND DISCUSSION

For ϕ-winding number n = 2, 3 and 4, Higgs modulus, magnetic charge density and energy density are plotted. Physical quantites investigated in this research involve the separation between one-monopole and half-monopole, d_z, magnetic dipole moment, μ_m, and total energy of the configuration, *E*.

The presence of a lower bound, λ_b, in FB among all solutions, though, appears to be unexpected, they share similar characteristics with the critical points, λ_c, whereby below which no numerical solutions can be found. In fact, λ_c are themselves a type of lower bounds. Thus, like the critical points, the lower bound, λ_b, for all FB must arise due to the natural properties of the solution. Both λ_b and λ_c for all solutions are tabulated in Table 1.

In 3D Higgs modulus plots, half-monopoles are located at the origin, extend towards the negative *z*-axis and show a string-like formation. The ‘t Hooft-Polyakov monopoles are located somewhere on the positive *z*-axis as shown in Figure 1(a). This is a standard multimonopole solution as the lowest point of Higgs modulus is located on the *z*-axis as indicated by the red circle. However, in Figure 1(b), the lowest point is deviated from the axis and it is a clear indication that this is a vortex ring solution. Both Figure 1(a) and Figure 1(b) are plots for ϕ-winding number n = 3 of HEB. In particular, Figure 1(a) is for λ = 3 and Figure 1(b) is for λ = 10.

Clearly, a transition from multimonopole solutions to vortex ring solutions occurred somewhere between λ = 3 and λ = 10. The exact transition points are also tabulated in Table 1 and similar transitions occurred in other branches and for different values of *n* as well.

A pattern can be observed from Table 1, transitions from multimonopole to vortex ring configuration will only occur for HEB and LEB for both n = 3 and 4. Transitions occurred earlier in HEB relative to LEB. However, no transition is observed in n = 4 NB, this new branch is a

vortex ring solution for the whole branch. Plots of Higgs Modulus, magnetic charge density and energy density of n = 4 NB are shown in Figure 2.

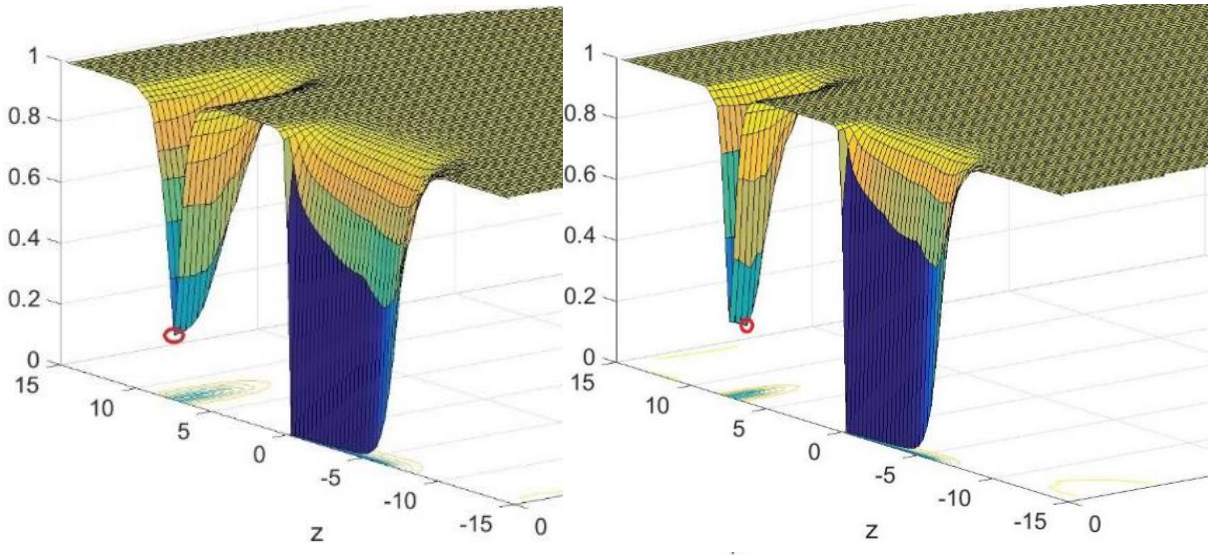

Figure 1. 3D Higgs modulus plots for n = 3 HEB (a) λ = 3, (b) λ = 10.

TABLE 1. Lower bounds, λ_b, critical point for bifurcation, λ_c, and transition point, λ_t, of the Higgs coupling constants, λ.

	n = 2 FB	n = 3 FB	n = 3 HEB	n = 3 LEB	n = 4 FB	n = 4 HEB	n = 4 LEB	n = 4 NB
λ_b	1.96	0.48	-	-	0.57	-	-	0.20
λ_c	-	-	2.28	2.28	-	2.87	2.87	-
λ_t	-	-	3.32	8.83	-	3.62	9.12	-

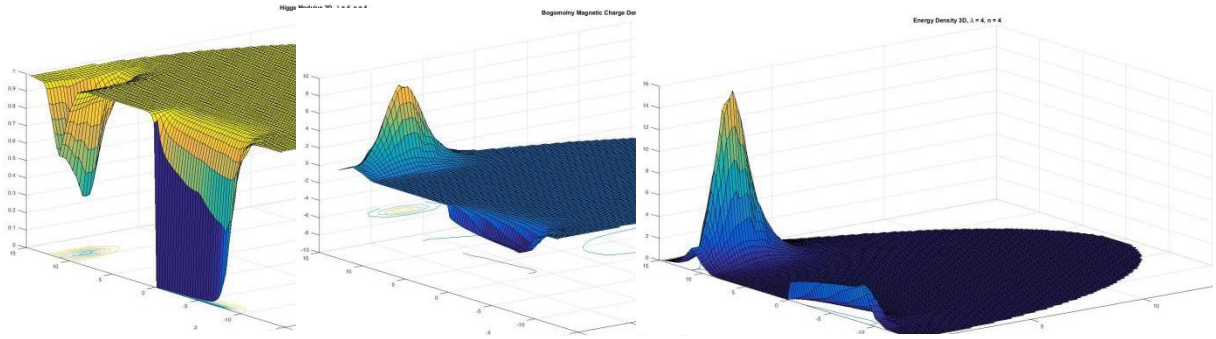

FIGURE 2. Plots of the new branch of n = 4 with λ = 4 for (a) Higgs modulus, (b) magnetic charge density and (c) energy density.

In Figure 2(a), the position of the lowest point of the Higgs modulus is a clear indication of vortex ring structure. The magnetic charge of 't Hooft-Polyakov monopoles and half-monopoles are of opposite sign are shown in Figure 2(b) with 't Hooft-Polyakov monopoles possess the positive charges. This feature is presented in all solutions. Plot of energy density is shown in Figure 2(c).

Plots of total energy versus $\lambda^{1/2}$ is presented in Figure 3. These plots show similar behaviours for n = 3 and 4 with the exception that there's one more branch (NB) for n = 4 as can be seen in Figure 3(b) and (c). For n = 2, however, the shape of the curve in Figure 3(a) is quite distinctive. It might indicate superimposing two half-monopoles would give rise to some unfamiliar physical

processes. In general, energy increases significantly with the change of n and energy continues to increase as the Higgs coupling constant, λ, increases.

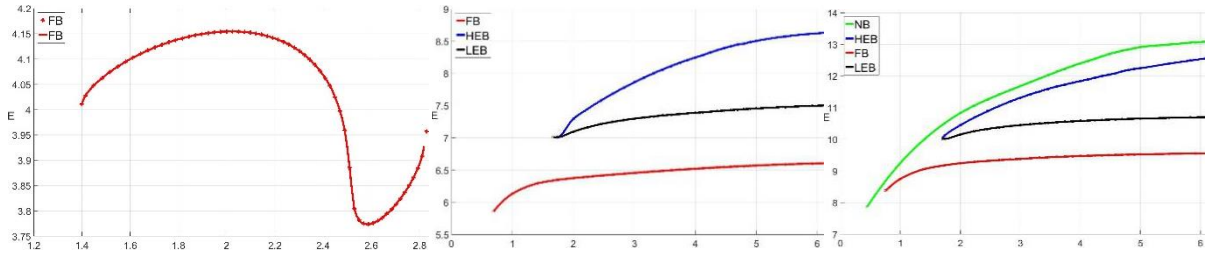

(a) (b) (c)

FIGURE 3. The plots of total energy, E versus $\lambda^{1/2}$, for (a) n = 2, (b) n = 3, (c) n = 4.

The magnetic dipole moment, μ_m, of all solutions are also plotted against $\lambda^{1/2}$ as shown in Figure 4. All solutions possess finite magnetic dipole moments and they tend to saturate at a certain point for both n = 3 and 4.

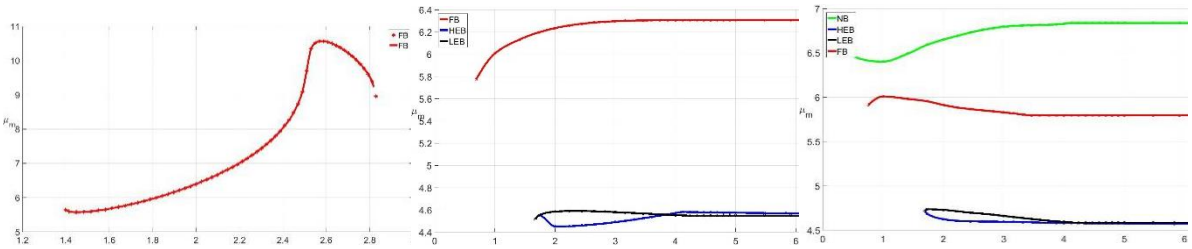

(a) (b) (c)

FIGURE 4. The plots of magnetic dipole moment, μ_m, versus $\lambda^{1/2}$, for (a) n = 2, (b) n = 3, (c) n = 4.

COMMENTS

As demonstrated above, there are bifurcating branchings which emerged for both n = 3 and 4 above the fundamental branch (FB, the red curve) with the blue curve being HEB and the black curve being LEB. For n = 4, however, a new branch appeared (green curve) with even higher energy. It is a vortex ring solution for the whole branching, no transitions occurred. Transitions from multimonopole solutions to vortex ring solutions occurred only for HEB and LEB of n = 3 and 4, λ_t are listed in Table 1. Lower bounds, λ_b are presented as well. Besides a lower bound, there exists an upper bound as well for n = 2 as shown in Figure 3(a).

ACKNOWLEDGMENT

The authors would like to thank School of Physics, Universiti Sains Malaysia.

REFERENCES

1. E.B. Bogomol'nyi and M.S. Marinov, *Sov. J. Nucl. Phys.* **23**, 355 (1976).
2. C. Rebbi and P. Rossi, *Phys. Rev.* **D22**, 2010 (1980); R.S. Ward, *Commun. Math. Phys.* **79**, 317 (1981).
3. P. Forgacs, Z. Horvarth and L. Palla, *Phys. Lett.* **B99**, 232 (1981); *Nucl. Phys.* **B192**, 141 (1981).
4. M.K. Prasad, Commun. *Math. Phys.* **80**, 137 (1981); M.K. Prasad and P. Rossi, *Phys. Rev.* **D24**, 2182 (1981).

5. G. 't Hooft, *Nucl. Phy.* **B79**, 276 (1974); A.M. Polyakov, *Sov. Phys. - JETP* **41**, 988 (1975); *Phys. Lett.* **B59**, 82 (1975); *JETP Lett.* **20**, 194 (1974).
6. B. Kleihaus and J. Kunz, *Phys. Rev.* **D61**, 025003 (2000); B. Kleihaus, J. Kunz, and Y. Shnir, *Phys. Lett.* **B570**, 237, (2003); B. Kleihaus, J. Kunz, and Y. Shnir, *Phys. Rev.* **D68**, 101701 (2003); *Phys. Rev.* **D70**, 065010 (2004).
7. Rosy Teh, B.L. Ng, and K.M. Wong, "Finite Energy One-Half Monopole Solutions of the SU(2) Yang-Mills-Higgs Theory", *Proceedings of Science, POS (ICHEP 2012)* 473; "Finite Energy One-Half Monopole Solutions", *Mod. Phys. Lett.* **A27**, (2012).
8. Rosy Teh, B.L. Ng, and K.M. Wong, "The One and One-Half Monopoles Solution of the SU(2) Yang-Mills-Higgs Field Theory", *Ann. Phys.* **343** (2014).
9. N.S. Manton, *Nucl. Phys. (N.Y.)* **B126**, 525 (1977).
10. A. Actor, *Rev. Mod. Phys.* **51**, 461 (1979).
11. K.G. Lim, Rosy Teh and K.M. Wong, *J. Phys. G: Nucl. Part. Phys.* **39**, 025002 (2012).